Transcranial ultrasonic imaging with 2D synthetic array

S.A. Tsysar, V.A. Khokhlova, O.A. Sapozhnikov
Physics Faculty
Moscow State University
Moscow, Russian Federation
sergey@acs366.phys.msu.ru

W. Kreider, V.A. Khokhlova, O.A. Sapozhnikov
Center for Industrial and Medical Ultrasound
Applied Physics Laboratory, University of Washington
Seattle, USA

V.D. Svet
Andreyev Acoustics Institute
Moscow, Russian Federation

A.M. Molotilov
AMM-2000
Moscow, Russian Federation

***Abstract*—In this work, an effective transcranial imaging technique is proposed to compensate for distortions of ultrasound (US) field caused by skull bone. The results of an experimental study using skull phantoms and 2D synthetic array are presented. The method was used to visualize mm-sized spherical scatterers made from styrofoam as well as a soft silicone tube mimicking a blood vessel. It is shown that the proposed technique is capable to compensate for field distortion and results in improved imaging through the skull.**

Keywords—transcranial imaging; skull phantoms; 2D synthetic array

I. Introduction

It is well known that ultrasound imaging of brain structures is significantly complicated by the presence of a skull, which is strongly inhomogeneous, reflective, and absorbtive. The relative effect of the skull bone on ultrasonic wave propagation can be mitigated by lowering the frequency to several hundreds of kHz, which has been also used in therapeutic ultrasound applications in brain [1,2]. At the same time, the use of higher frequencies (above 1.5 MHz) is of particular interest to achieve the requisite image resolution. In order to accurately compensate for field distortions, signals scattered in different directions should be captured. Numerous trials by different groups [3–6] have been based on modeling and measurements involving linear phased arrays, which are capable of compensating for distortions introduced by a 1D layer of a curved bone. However, real skulls introduce distortions along a 2D surface; consequently, a linear array cannot provide adequate imaging because waves scattered out of the imaging plane are missed.

Another critical problem is how to characterize acoustic properties of the skull, which is required for calculating the phase and amplitude deviations of the transmitted and reflected acoustic signals during transcranial imaging procedure. Various methods have been developed for determining skull profiles: definition of the parameters of skull bones can be performed by computed tomography (CT) [7] or using phase conjugation of the acoustic field in the presence of a strong scatterer inside the skull [8]. In the case the biopsy has been made, interstitial technique with MR guidance is applicable [9]. Direct acoustic methods as those used in nondestructive testing (NDT) are also available [3-5]. Current work is concentrated on developing an ultrasound-based noninvasive method for transcranial imaging, therefore, MRI or CT skull profiling methods are not of the interest because they are applicable for transcranial imaging themselves, not only bone characterization. These methods are well-developed and useful in combination with ultrasonic for therapeutic procedures. In case of diagnostics, combination of different methods may significantly complicate the procedure. Thus, acoustic methods for bone profiling are preferred for transcranial ultrasonic imaging. In the previous work [10] we proposed enhanced nonlinear technique which also can be used. In the current paper, conventional echo-pulse technique was used as an alternative method.

II. Method and Materials

Our approach utilizes a virtual 2D array, which is synthesized by mechanical translation of a focused broadband transducer (2 MHz central frequency, Panametrics NDT, aperture 1", focal distance 3") by a computer-controlled positioner (Precision Acoustics UMS3). To mimic small array elements positioned on the skull, the transducer's focus is scanned point-to-point along the proximal surface of the bone phantom. Skull phantom was made using the same components as has been described in the previous publication [10]. In the experiment, the phantom was placed between the ultrasonic transducer and scatterers in a water tank filled with degassed filtered water (Precision Acoustics Water Treatment System). Target objects were high-contrast mm-sized spherical scatterers made from styrofoam and a soft silicone tube mimicking a blood vessel. A generator (Agilent 33210A) produced a signal having a form of one or two cycles of the central frequency. The transducer radiated acoustic pulse, which propagated toward the scatterers through the skull phantom. Acoustic reflections from the scatterers and the skull were received by the same transducer for each node of the synthetic array and were averaged using an oscilloscope

RSF №14-15-00665 and NIH R21EB016118.

software (Tektronix TDS 5054B). Averaging over 2048 waveforms at each spatial point gave higher signal-to-noise ratio and increased the dynamic range of the ADC system up to 13 bits. After scanning over all points, the collected signals were used for an imaging procedure, which consisted of several steps. At the first step, the spatial profile of the skull bone was extracted, then correction coefficients for the phase compensation were calculated based on the previous step and, at the final stage, construction of the image of objects located behind the skull phantom was accomplished.

A. *Skull Bone Profiling*

It should be noted, that the detection of the external and internal surfaces of the skull was also performed in several stages. First, the intensity thresholds for each interface were determined on the B-scan. Then, for each node of the 2D synthetic array the signal values that exceeded the thresholds were determined. Spatial filtering based on correlation factor calculation of the resulting three-dimensional arrays for both surfaces was the next step. The final step was an interpolation of the two surfaces based on the radial basis functions (RBF).

B. *Distortion Compensation*

Experimental data obtained for reconstructing the bone shape were used to calculate the correction factors. An image correction algorithm was based on the raytracing method. In the first approximation, all acoustic paths from the elements of the 2D array to each point of the future image were divided into different sections: in front of the skull phantom (red lines in Fig.1), inside the phantom (green lines), and behind the skull (blue lines). Note that Fig.1 shows illustrative sparse paths (approx. 5% of array are shown) for only one point of the reconstructed image; distal (flat) surface of the skull phantom is not shown. Amplitude and phase correction procedure was based on the known values of the sound speed and absorption coefficient for the different path sections.

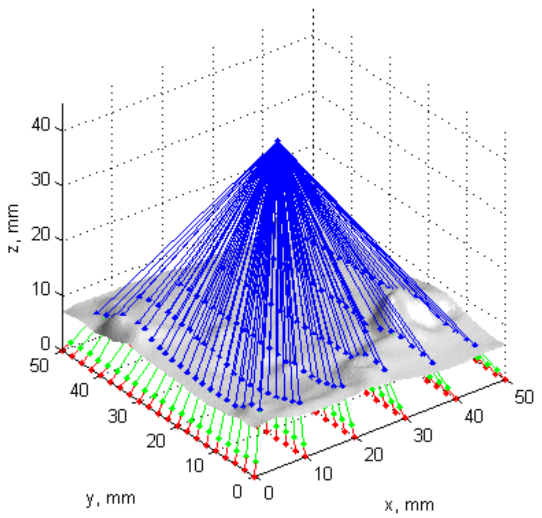

Fig. 1. Illustrative paths representation for one image point. The distal flat surface of the phantom is not shown. Color of the path section refers to the propagation medium: outside the skull (red), inside the skull phantom (green), and behind the phantom (blue).

C. *Image Formation*

After correction of the amplitude and phase at all array elements, the transcranial image formation was similar to the B-scan formation. First, the measured waveforms of each array element were filtered, then the resultant signals were summed with the delays that corresponded to the location of the chosen image point in 2D or 3D representation. The final step was the calculation and visualization of the waveform envelopes along the z (in-depth) direction.

Using this approach it was possible to determine the skull profile over the scanning region and to use these data for imaging objects placed behind the skull.

III. RESULTS

After series of experiments, the images of different scatterers placed behind the phantoms were obtained. Phantoms with various composition, thickness and curvature were employed. In the current section, the typical results are presented. Consider a skull phantom layer with one flat and one curved surface as shown in Fig. 2a. Red square represents a 4x4 cm scan region.

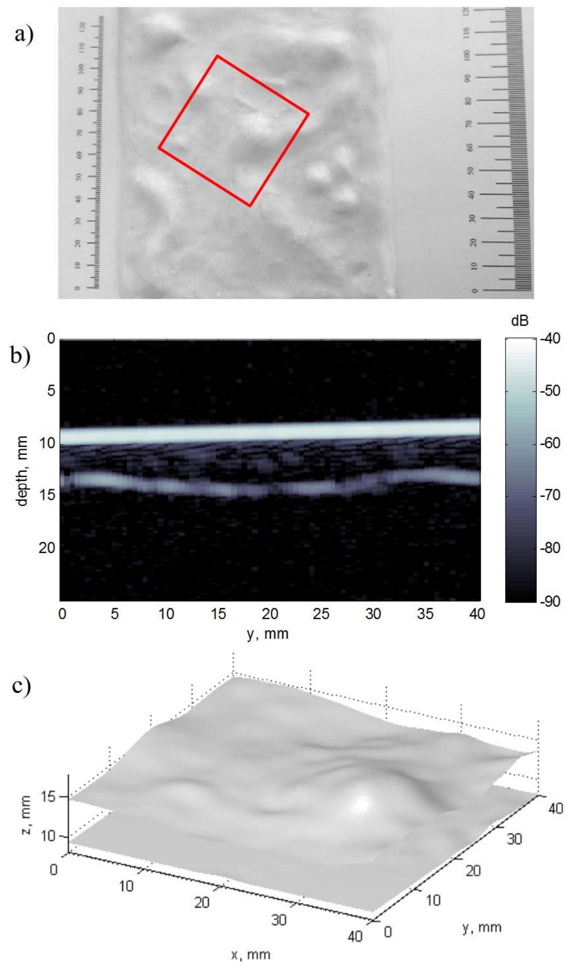

Fig. 2. (a) Photo of the skull phantom with marked 4x4 cm scan region, (b) one of B-images in ZY section, (c) reconstructed 3D surfaces of the skull bone phantom.

After measurement procedures described in the previous section, a set of B-scans (Fig. 2b) and full extracted profile of the skull phantom (Fig. 2c) were obtained. These results allowed to image a single or distributed scatterers with the distortion compensation.

Figure 3 illustrates the reconstruction results for two 3-mm diameter spherical scatterers (left column) and a 4-mm diameter silicone tube mimicking a blood vessel with two 2-mm diameter spherical scatterers (right column): a) behind the skull phantom without correction, b) behind the skull phantom with correction, and c) reference without skull phantom. It is clearly seen that even simple raytracing compensation approach applied to the 2D phased array can significantly reduce image distortions caused by the presence of the skull phantom. Two spherical scatterers were hardly resolved before correction. After distortion correction they are clearly seen, transversal size is close to 3 mm and comparable with reference. Smaller scatterers on the tube also became better resolved and localized, transversal size was decreased to 2–4 mm from 4–6 mm. Tube mimicking a blood vessel is better resolved after the correction procedure. On all images lateral resolution is not sensitive to correction because it is determined by duration of probe pulse.

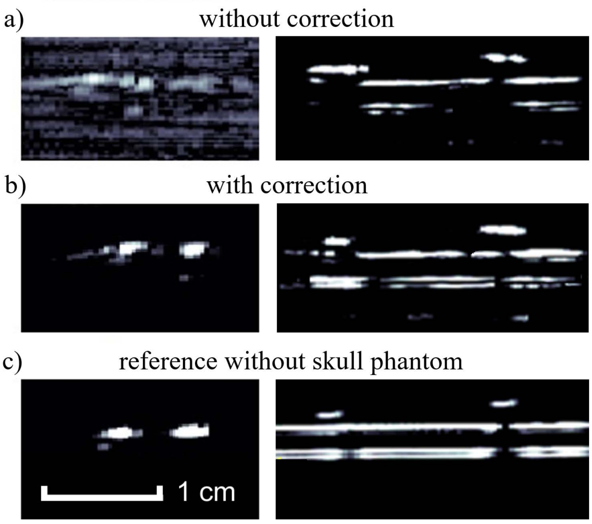

Fig. 3. Imaging of two 3 mm spherical scatterers (left column) and 4 mm silicone tube mimicking blood vessel with two 2 mm spherical scatterers on it (right column).

IV. Conclusions

The proposed method was used to image both mm-sized spherical scatterers made from styrofoam and a soft silicone tube mimicking a blood vessel. The image formation algorithm included measurement of the skull profile as the first step; the corresponding correction was based on the raytracing method. The technique clearly compensates for field distortion resulting in improved imaging through skulls. The results of this study show the possibility of developing a 3D transcranial US imaging system with the use of 2D arrays.

Acknowledgments

Work was supported by RSF №14-15-00665 and NIH R21EB016118.

References

[1] P. Ghanouni, K.B. Pauly, W.J. Elias, *et al.*, “Transcranial MR-guided focused ultrasound: a review of the technology and neuro applications,” AJR Am. J. Roentgenol., vol. 205(1), pp. 529-551, 2015.

[2] M. Pernot, E. Bossy, M. Muller, *et al.*, “Experimental and numerical investigation of ultrasonic transmission through the skull bone and associated temperature rise,” J. Acoust. Soc. Am., vol. 123, p. 3513 2008.

[3] A. Wydra, E. Malyarenko, K. Shapoori, and R.G. Maev, "Development of a practical ultrasonic approach for simultaneous measurement of the thickness and the sound speed in human skull bones: a laboratory phantom study," Phys Med Biol., vol. 58(4), p. 1083, 2013.

[4] S.V. Baykov, A.M. Molotilov, and V.D. Svet, “Physical and technological aspects of ultrasonic imaging of brain structures through thick skull bones: 1. Theoretical and model studies,” Acoust. Phys., vol. 49, p. 276, 2003.

[5] S.V. Baykov, L.V. Babin, A.M. Molotilov, *et al*. “Physical and technical aspects of ultrasonic brain imaging through thick skull bones: 2. Experimental studies,” Acoust. Phys. Vol. 49, p. 389, 2003.

[6] K. Shapoori, J. Sadler, A. Wydra, *et al*., “An ultrasonic-adaptive beamforming method and its application for trans-skull imaging of certain types of head injuries; part I: transmission mode,” IEEE Trans. Biomed. Eng., vol. 62(5). pp. 1253-1264, 2014.

[7] J.-F. Aubry, M. Tanter, M. Pernot, J.-L. Thomas, and M. Fink, “Experimental demonstration of noninvasive transskull adaptive focusing based on prior computed tomography scans,” J. Acoust. Soc. Am., vol. 113, p. 84, 2003.

[8] J.-L. Thomas, and M. Fink, “Ultrasonic beam focusing mirror: application to transskull therapy”, IEEE Trans. Ultrason. Ferroelec. Freq. Contr., vol. 43, p. 6, 1996.

[9] M. Canney, F. Chavrier, S. Tsysar, *et al.*, “A multi-element interstitial ultrasound applicator for the thermal therapy of brain tumors,” J. Acoust. Soc. Am., vol. 134(2), pp. 1647-1655, 2013.

[10] S.A. Tsysar, A.V. Nikolaeva, V.D. Svet, *et al.* “Experimental study of transmission of a pulsed focused beam through a skull phantom in nonlinear regime,” AIP Conf. Proc., vol. 1685, pp. 040013–1-4, 2015.